Fermi National Accelerator Laboratory

FERMILAB-Pub-85/160-A
November 1985

Neutrinos in High-Energy Astrophysics *

CHRISTOPHER T. HILL
Fermi National Accelerator Laboratory, P.O. Box 500
Batavia, Illinois, 60510

and

DAVID N. SCHRAMM
Departments of Astronomy and Astrophysics,
Physics and EFI
The University of Chicago
Chicago, Illinois 60637
and
NASA/Fermilab Astrophysics Center, Fermilab

and

TERRY P. WALKER
NASA/Fermilab Astrophysics Center, Fermilab
and
Astronomy Department
Indiana University
Bloomington, Indiana 47405

Abstract

We discuss both diffuse cosmic ray neutrinos produced as secondaries by nucleon and $3^{o}K$ microwave background collisions and the flux expected from typical high energy gamma ray sources, specifically Cygnus X-3. We consider the feasability of detecting these fluxes and the implications of such observations.

*Contribution to the Festschrift of Saburo Miyake

I. Introduction

The existence of ultra-high energy cosmic ray neutrinos may have important consequences for our understanding of cosmic ray sources and the behavior of various astrophysical systems. We consider presently two extremes, the "old" neutrinos that are produced as very energetic nucleons collide with the microwave background and photoproduce, and the "new" or prompt neutrinos associated with specific galactic sources, in particular Cygnus X-3.

The old neutrinos may be predominantly associated with very large redshift objects such as QSO's if the cosmic ray activity of these objects follows the apparent increase in luminosity. The neutrinos arrive by line of sight while the nucleons are undergoing a random walk on the cluster scale, and thus the neutrino spectrum may contain important information about the early phase of galactic evolution. Here we review the recent results of the Fly's Eye experiment that suggest the existence of the Greisen cut-off and consider the detectability of the associated neutrinos in this bright phase model, as previously discussed by Hill, Schramm, and Walker.[1,2]

The possibility of detecting a point source of >Tev neutrinos in underground proton decay detector has stimulated a great deal of excitement in the past year. Several groups have calculated the neutrino flux and resultant muon event rates in large underground detectors that can be expected from a class of Tev gamma-ray sources.[3] In Section III we discuss the explicit calculations found in the analysis of Kolb, Turner, and Walker[4] for the X-ray binary system Cygnus X-3.

II. Implications of the Greisen Cut-off

Recently the Fly's Eye experiment has presented data on the ultra-high energy cosmic ray spectrum[4,5] in which there is strong evidence of a spectral flattening above 10^{19}ev from a differential index of 2.94±.02 to 2.42±.27. Above 7×10^{19}ev there is evidence of a cut-off. Though it is true that the detector acceptance is energy dependent and, of course, this data consists of only 62 events, nonetheless this structure survives numerous experimental self-consistency checks (for example, the shape remains if cuts with range from the center of the detector are made on the data). It should be noted that, except for the last few highest energy bins, the Fly's Eye results are in general accord with those of Haverah Park.

As is well known, shortly after the discovery of the 2.7°K microwave background radiation, Greisen[6] and independently Kuzmin and Zatsepin[7] remarked that above energies of order 7×10^{19}ev the intergalactic medium must become opaque to protons on scales of tens of Mpcs, due to photomeson production. Stecker, Berezinsky and others[8] gave the first accounts of this mechanism using experimental laboratory data. Nonetheless, there has not been incontrovertible evidence for the Greisen-Zatsepin cut-off until the Fly's Eye's new results. The implication of this is then striking: the UHE cosmic rays must be extra-galactic and have traversed at least a few interaction lengths (~20 Mpc).

Previous analyses were essentially "zeroth moment" approximations to the actual transport evolution of the spectrum in traversing the microwave background. In the past two years we undertook a much more detailed analysis involving the direct integration of the photomeson

production Ginzburg-Syrovatsky equation[1]. We were surprised to see several new effects appropos an $E^{-2.5}$ injection spectrum. We note (i) the recoil protons are not thrown to arbitrarily small energies but rather accumulate immediately below the cut-off in a range of order $3x10^{19}$ev to $6x10^{19}$ev; (ii) with much greater range (exceeding 100Mpc) there onsets a dip at 10^{19}ev due to the peaking of energy losses due to e^+e^- pair production (this analysis was based upon Blumenthal[9]). (iii) By 3000 Mpc (the Hubble range) the spectrum cut-off has fallen to $\sim 10^{19}$ev.

The observed bump in the Fly's Eye data cannot be interpreted as the recoil proton pile up of the $E^{-3.0}$ spectrum. This follows simply by considering the total number of events above 10^{19}ev which is 62 compared to ~40 expected for an $E^{-3.0}$ pile-up. Thus one is seeing one of two possible phenomena: (i) the emergence of a flatter extra-galactic component which is crossing over the steeper, presumably galactice $E^{-3.0}$ spectrum seen below 10^{19}ev or (ii) the pile-up of an arbitrary injection spectrum above $E\sim10^{20}$ev, e.g. a monoenergetic spike of a sufficiently distant object after several interaction lengths can produce this structure.

It is reasonable that up to energies of order 10^{19}ev we are seeing primarily a galactic spectrum, possibly Fe-group rich, which is governed by an injection spectrum and a diffusion trapping time which is energy dependent. Thus the observed galactic spectrum would follow an $E^{-\gamma_i}t(E)$ shape and for the sake of argument we shall assume $\gamma_i=2.5$ and $t(E)\sim E^{-.5}$. The spectrum outside the galaxy is not trapped, but is essentially line of sight (or "trapped" on a scale of the age of sources or age of the Universe) and will therefore have the form $E^{-\gamma_i}$. Thus at some energy we

may expect a crossover from the steeper galactic spectrum to the flatter extragalactic one.

Assuming all galaxies are roughly equivalent to our own, that an extra-galactic crossover occurs at 10^{19}ev, and that contributing sources range out to some distance L, we may estimate L. We take for the normalization of the universal injection spectrum the observed CR spectrum at 10^{16}ev. Then, for an idealized disk structure of our galaxy (the solar system on the periphery) we obtain the local flux:

$$J_L = \omega d \rho_s \eta_s \, (E_o/E)^{\gamma_i} \, (E_o/E)^{.5} \tag{1}$$

where ρ_s is the galactic source density, η_s is the activity per source (particles/time), d the width of the galaxy and ω a geometric factor of order unity. The sum over extragalactic sources to distance L then gives:

$$J_E = \int_0^L \rho_s \eta_s \, (\pi R^2 d) \rho_G \, (E_o/E)^{\gamma_i} \, dl$$

$$= \rho_s \eta_s \rho_G L \, (\pi R^2 d)(E_o/E)^{\gamma_i} \tag{2}$$

where ρ_G is the density of galaxies ($\sim .03/\mathrm{Mpc}^3$), and R the galactic radius ($\sim$10kpc). Thus, equating these fluxes at 10^{19}ev gives L:

$$L \sim \omega/(\pi R^2 \rho_G) \, (E_o/E')^{.5} \tag{3}$$

where E' is $\sim 10^{19}$ev. If we assume $\gamma_i = 2.5$ then L is of order 100 Mpc. This corresponds to between 15 and 20 interaction lengths (i.l.; 1i.l. = 6Mpc). We emphasize that this model will have the dominant contribution due to sources at L. Thus, superimposing the 15 to 20 i.l. curves upon an $E^{-3.0}$ spectrum gives the composite seen in Fig.(1).

In this model we have assumed that the dominant contribution below 10^{19}ev is given by relatively local extragalactic sources. In ref.(5) we assumed the dominant contribution below 10^{19}ev is given by distant, large redshift sources. In the latter case we predicted a dip should occur at 10^{19}ev because such distant sources would be cut-off at that energy and the cross-over energy is emphasized (it may be possible to consider other linear combinations in which the dip would be reduced). Evidence from the Fly's Eye with relatively good statistics does not indicate a dip; we therefore believe that Hillas-Blumenthal models in which the spectrum below 10^{19}ev is large red-shift cosmological in origin are disfavored.

We emphasize that the pile-up structure can also be due to an arbitrary initial injection spectrum, such as a delta-function "spike" above $\sim 10^{20}$ev, accumulating below the cut-off[1,10].

The composite spectrum of Fig.(1) is in good agreement with the Fly's Eye data for the simple model considered. L is a typical scale for the local supercluster. The abundance should swing from a galactic composition below 10^{19}ev to a principally proton rich spectrum at the peak of the bump. This prediction would seem to be universally true for even an iron rich injection spectrum. The anisotropy would seem to be associated with the local supercluster in this model. It is very difficult in any model with a Greisen cut-off to understand a galactic

associated anisotropy to our knowledge (it would be of considerable interest to consider local steering of an incoming extra-galactic spectrum; evidently some anisotropy of the extragalactic spectrum would be required).

If the Fly's Eye bump above 10^{19} eV is a bare measurement of the extragalactic cosmic ray component, it can be used to calculate the flux of ultra-high energy neutrinos necessarily arising from the photomeson production causing such a feature. The cosmic ray spectrum measured by Fly's Eye above 10^{19} eV is best fit by a power law of the form:

$$J_N(E) = a\,(E)^{-\gamma_i}\ ; \qquad \begin{cases} a = 34\pm17\ \text{Eev}^{-1}\text{km}^{-2}\text{sr}^{-1}\text{yr}^{-1} \\ \gamma_i = 2.47\pm0.27 \end{cases} \tag{4}$$

with a cut-off above 7×10^{19} eV. The resultant integrated extragalactic flux above 10^{18} eV is then:

$$I_N(>10^{18}\ \text{eV}) = a/(\gamma-1) = 23.9\pm12.8\ \ \text{km}^{-2}\text{sr}^{-1}\text{yr}^{-1} \tag{5}$$

Following the analysis of ref.(5), the minimum neutrino flux associated with these cosmic rays is:

$$I^{min}_{\nu_e}(>0)/I_N(>10^{18}\text{eV}) = c(\gamma_i, E_o)/2 \tag{6}$$

and:

$$J^{min}_{\nu_e}(E) = (2.04\text{x}10^{-4}\ I_N(>10^{18}\text{eV}))\ J^{min}_o(E) \tag{7}$$

where $c(\gamma_i, E_0) \sim 4.35\times10^{-3}$ for $\gamma_i=2.5$ and the differential neutrino spectrum, $j_0(E)$, is shown in Fig.(3). Combining Eqs. (5)-(7) we have for the minimum neutrino flux:

$$I^{min}_{\nu_e}(>10^{18}eV) = (52.1\pm27.9)10^{-3}\ km^{-2}sr^{-1}yr^{-1} \tag{8}$$

and:

$$J^{min}_{\nu_e}(E) = (4.9\pm2.6)x10^{-3}\ J^{min}_{o}(E) \tag{9}$$

We say "minimum" because we have not yet scaled the flux by a factor R_H/L which takes into account the fact that we see neutrinos from photomeson production at Hubble length scales while only sampling cosmic rays originating from the scale L. For the same reason, there can be an enhancement of the neutrino spectrum relative to the cosmic ray spectrum due to bright phase scenarios of galactic evolution.

We envision two possible methods for the detection of such an ultra-high energy neutrino flux. An EAS detector, like the Fly's Eye, would look for upward going air showers produced by these neutrinos after passing thru the earth, while the DUMAND detector could see these neutrinos as contained interactions in $10^{14}cm^3$ of sea water.

In both cases, the event rate is given by:

$$\Gamma(yr^{-1}) = \int J_{\nu_e}(E)A_{eff}P(E)\ S(E,\Omega)\ dE\ d\Omega \tag{10}$$

Here A_{eff} is the effective cross sectional area the detection region presents to incoming neutrinos ($\sim10^2km^2$ for Fly's Eye and $\sim0.1\ km^2$ for

DUMAND), P(E) is the probability that a neutrino passing the detection region interacts with a nucleon:

$$A_{eff}P(E) = A_{eff}\langle L_{det}\rangle/L_{\nu N} \sim 10^{-6}\, \sigma_{34}(E)\ km^2 \tag{11}$$

for both Fly's Eye and DUMAND (here $\langle L_{det}\rangle$ is the average linear dimension of the detection region (m.w.e.), $L_{\nu N} \sim 10^{8}/\sigma_{34}$ m.w.e., and we have taken $\sigma_{34} \equiv \sigma/10^{-34}cm^2 \sim \ln E_{Tev}$. For $s \gg M_W^2$ ($E_\nu \gg M_W^2/2m_N \sim 3.6$ TeV), the total νN cross section is given by:

$$\sigma_{\nu N} = \sigma_{\bar{\nu}N} = \frac{G_F^2}{(2\pi)} M_W^2 \ln\left(\frac{s}{M_W^2}\right) \sim \left(6\times10^{-35}\right)\ln\left(\frac{E_\nu}{3.6TeV}\right) cm^2 \tag{12}$$

which for the EeV energies considered here has the approximate value $\sigma_{\nu N} \sim 7\times10^{-34}\ cm^2$. $S(E,\Omega)$ is a factor which accounts for shadowing of the neutrino flux by the earth:

$$S(E,\Omega) = e^{-n\sigma L} = e^{-\alpha(E)\cos(\theta)};\quad \alpha(E) = .3\sigma_{34}(E) \tag{13}$$

where L is the slant depth of the incoming neutrino and θ is the angle between $\vec{L}$ and detector zenith. Integration of S over the earth (assuming $\sim 2\pi$ detector coverage) yields a factor $2\pi(1-e^{-\alpha})/\alpha$. The upward and downward (S=1) rates are given by:

$$\Gamma(yr^{-1}) = \begin{cases} (2\times10^{-5}) \int_{E_o}^{E} J_{\nu_e}(E)\,(1-e^{-\alpha})\,dE & \text{(upward)} \\ (6\times10^{-6}) \int_{E_o}^{E} J_{\nu_e}(E)\,\sigma_{34}(E)\,dE & \text{(downward)} \end{cases} \tag{14}$$

the upward rate corresponding to Fly's Eye and the sum of downward and upward rates corresponding to DUMAND.

In accordance with Fig.(2), we approximate the bright phase neutrino spectra as

$$J^{BP}_{\nu_e}(E) \sim A^{BP}(\bar{z})\ J^{min}_{\nu_e}(E)/E^3 \tag{15}$$

where the bright phase normalization, $A^{BP}(\bar{z})$, takes values of $\sim 10^2$, 10^4, and 10^6 for $\bar{z} \sim 2$, 4, and 7 respectively, and $j^{min}_{\nu_e}(E)$ is taken to be a step function in energy (the larger $\bar{z}$ calculations are normalized at 2×10^{17}eV). With these approximations, the interaction rates take the following form:

$$r(yr^{-1}) = \begin{cases} \text{Minimum} & ; \quad \text{Bright Phase} \\ 2\times10^{-5} I_V(E_0) & ; \quad 10^{-7} A^{BP}(\bar{z}) \int_{E_0'}^{E_c} \frac{(1-e^{-\alpha})}{E^3}\, dE \quad \text{(upward)} \\ 8.4\times10^{-5}\left[I_V(E) + 3.6\times10^{-4}\int_{E_0}^{E_c} E\, dE\right]; & 3\times10^{-8} A^{BP}(\bar{z}) \times \int_{E_0'}^{E} \sigma_{34}(E)\, dE/E^3 \quad \text{(downward)} \end{cases} \tag{16}$$

In Table I we give a compilation of these rates. In calculating the bright phase rates we have taken into account that A_{eff} decreases by a factor of ~70 when E_o' is taken to be 2×10^{17}eV. We see that, in most cases, the yearly rate of Fly's Eye bump neutrino interactions is not observable, but the rates can be brought into the observable regime by including galactic evolution effects with the epoch of maximum activity occurring at $\tilde{z}\geq 6$ along with extending the incoming neutrino energies down to 2×10^{17}eV. We point out that the event rates listed are somewhat uncertain but that this "bright phase threshold" is accurate to $\tilde{z}\pm1$. In addition there is an upper bound to $\tilde{z}$ from the diffuse X-ray background at $\tilde{z} \sim 7$ for the $1/E^3$ bright phase spectra.

Presently we comment upon the astrophysical implications of detectable neutrinos as described by these models. The validity of "bright phase" models may well rest with the determination of the shape and evolution of the luminosity function for quasars (QSO's) and the epoch of galaxy formation. If extragalactic cosmic ray (EGCR) production is associated with active galactic nuclei (AGN) then one would expect large z enhancements in EGCR fluxes to be reflected in the evolution of the average co-moving luminosity of young QSO's. There is some evidence that although the total number of QSO's per co-moving volume decreases with increasing z[11], the increase in the number of bright QSO's is such that $\langle L\rangle_{co\text{-}moving}$ increases with increasing z[10]. We should point out that limits on the X-ray production of young QSO's indicate a cut-off in the increase of $\langle L\rangle_{co\text{-}moving}$ at a z_{max} of ~5[12]. However, one might also expect enhancements in EGCR production during the epoch of galaxy formation. Optical searches designed to look for the continuum emission from these primeval galaxies (large redshift

galaxies in the throes of initial star formation) indicate galaxy formation occuring at $z > 5$[13]. In any case the observation of a flux of 10 EeV neutrinos would be an indication of robust cosmic ray production in the past and could possibly open a new window to the early history of galactic evolution.

III. (a) The Cygnus X-3 System

The Cyg X-3 system is a very robust source of radio, infrared, X-rays, medium energy (ME) γ-rays (~100 MeV), and ultra-high energy (UHE) γ-rays (> TeV) photons. A 4.8^h period is observed in all but the radio emission and appears to be associated with the orbital period of a binary system, thought to consist of a young pulsar and ~4 $M_\odot$ companion.[14,15] Eclipsing of the pulsar by the companion is believed to be responsible for the observed periodicity (see Fig. 3).

Characteristics of the light curves from Cyg X-3 allow one to construct models of the system. The X-ray light curve does not contain a zero flux minimum but instead is smoothed to a sinusoid.[14] The absence of a complete X-ray eclipse can be understood if the binary system is shrouded by a cocoon of optical depth unity for X-rays, which scatters X-rays originating from the pulsar during eclipse.[16,17] ME γ-rays from the pulsar pass directly through the cocoon without being scattered, resulting in the zero flux minimum (centered about X-ray minimum which we take to occur at phase $\psi = 0$) observed by Lamb et al.[18] at ~100 MeV. The duration of the eclipse ($\Delta\psi \approx 40\%$) and the orbital period establishes an upper limit for the companion mass of $4M_\odot$, assuming a $1.4M_\odot$ pulsar.

Although the UHE γ-ray light curve exhibits a 4.8^h period, it is much different in structure than those observed in IR, X-ray, and ME γ-ray, suggesting a different mechanism for the UHE photon production. The UHE γ-ray light curve seems to show 2 pulses, occurring just before and just after X-ray minimum separated by 0.4 in phase, and having a width $\Delta\psi \lesssim 0.05$. The mean UHE γ-ray flux above 2 TeV in the pulses is $\sim 10^{37}$ erg/sec[19-21]. In addition, a 4.8^h periodic signal from Cyg X-3 has been detected in the energy range 2×10^{15} to 2×10^{16} eV by Samorski and Stamm[22] and Lloyd-Evans etal.[22]. Their data, combined with lower energy measurements, can be fit by a power law spectrum:

$$dN_\gamma/dE_{TeV} \approx 3\times10^{-10} E_{TeV}^{-2.1} \text{ cm}^{-2} \text{ sec}^{-1} \qquad (17)$$

for the average photon flux. The uncertainty in the slope is 2% and in the normalization a factor of 2. Assuming isotropic emission and a distance of 12 kpc,[10] the luminosity of Cyg X-3 above 1 GeV is $\sim 10^{38}$ erg sec^{-1}, making it the brightest γ-ray point source in the galaxy.

Vestrand and Eichler[15] have proposed the following model for the UHE γ-ray flux from Cyg X-3. The pulsar is a source of UHE protons which collide with the companion star, producing π^o's whose subsequent decays lead to UHE photons. If the region of neutral π production is optically thin to TeV photons, they can pass through the companion and are observed. Only for a small fraction of the orbital phase, around the time that line-of-sight to the pulsar just grazes the companion star ($\psi \approx \pm 0.25$)[11], are both of these conditions met--sufficient material to produce π^o's and optical depth from the production site to the

observer of less than order unity, thereby accounting for the two narrow UHE γ ray pulses which are observed.

In addition to making π^o's, pN interactions in the companion will also produce $\pi^{\pm}$'s whose decays result in a ν_μ flux from the system.[15,25] In this paper we will discuss the characteristics of the neutrino flux from Cyg X-3 and the possibility of detecting these neutrinos in large, underground detectors.[26]

(b) High Energy Neutrino Production in Cyg X-3

In this section we use the UHE photon spectrum to calculate the spectrum and phase diagram of the neutrinos that also must be produced. The origin and spectrum of the incident proton beam is irrelevant for our purposes. We need only assume that π^o, π^+ and π^- are produced in equal numbers.

If the UHE γ-rays originate from a source spectrum of the form

$$\frac{dS_\gamma(E_\gamma)}{dE_\gamma} = AE^{-n} \quad , \tag{18}$$

and are produced by π^o decays, then the π^o source spectrum is inferred to be

$$\frac{dS_{\pi o}(E_\pi)}{dE_\pi} = A\, 2^{n-2} E^{-n} \tag{19}$$

where the factors of 2 come from counting 2 photons of energy $E_\pi/2$ from each π^o decay. There should also be π^+'s and π^-'s produced in numbers

comparable to π^o, and $dS(\pi^+ + \pi^-)/dE = 2dS_{\pi^o}/dE$.

The $\pi^\pm$ decays will produce neutrinos with an energy that depends upon whether the $\pi^\pm$'s decay in flight, or interact before decay. For the moment we will assume the $\pi^\pm$'s decay in flight, and later we will discuss the conditions under which the $\pi^\pm$'s interact before decay. K mesons will also be produced by the proton interactions, however at only about 10% of the rate at which $\pi^\pm$'s are produced. Their decays will also produce ν_μ's.

The decay of a $\pi^\pm$ in flight produces a neutrino of energy $E_\nu = E_\pi(1-m_\mu^2/m_\pi^2)/2$, which leads to a neutrino source spectrum of[27]

$$\frac{dS_\nu(E_\nu)}{dE_\nu} = \frac{(1-m_\mu^2/m_\mu^2)^{n-1}}{2} \frac{dS_\gamma(E_\gamma)}{dE_\gamma} \quad . \tag{20}$$

In order to relate the source spectrum to the observed number spectrum it is necessary to propagate the source spectrum through the companion star. The absorption of the γ's and ν's by the star depends upon the column density material encountered by the γ or ν traversing the star, which in turn depends upon the phase ψ.[24]

The photons can only traverse the star when the source is near phase $\psi \approx \pm 0.25$. Since the γN cross section at high energies is roughly energy independent, the relative intensity of the UHE photon flux should be energy independent, and appear only at phase $\psi \approx \pm 0.25$. The UHE photons are detected for a total phase of $(\Delta\psi)_\gamma \approx 0.05$. Although a normal stellar model would result in $(\Delta\psi)_\gamma$ at least a factor of 10 smaller, the companion star in this system is expected to be

significantly altered by the compact object,[15] which can easily account for the large $(\Delta\psi)_\gamma$.

Due to their weak interaction cross section neutrinos more easily traverse the star. However, very energetic neutrinos are not able to traverse the star around phase $\psi=0$, and the phase diagram for UHE neutrinos will also show an eclipse. Unlike the photons, the neutrino cross section is energy dependent, and the phase diagram (or 'light curve') for neutrinos will reflect this energy dependence.

The incident neutrino beam is reduced while traversing the star by a factor of $\exp(-\int \sigma n(x)dx)$, where σ is the total cross section for muon production, $\nu_\mu N \rightarrow \mu X$ and n is the number density of nucleons. At energies below about 100 TeV, the cross section increases linearly with energy, and above 100 TeV the cross section increases only logarthmically, due to the effect of the W-boson propagator,[28]

$$\sigma = 7\times10^{-36} E_{TeV}\ cm^2 \qquad E \lesssim 100\ TeV \tag{21a}$$

$$\sigma = 1.2\times10^{-34} \ell n\ E_{TeV}\ cm^2 \qquad E \gtrsim 100\ TeV \tag{21b}$$

At energies below 100 TeV the antineutrino cross section is one half this value, while at energies above 100 TeV the two cross sections are roughly equal. We estimate $\int n(x)dx$ by assuming that the companion star has a radius of $R = 2\ R_\odot$, a central density of 30 g cm^{-3}, and a density profile given by: $\rho(r) = \rho_c \exp(-12r/R)$. We find that neutrino absorption is more sensitive to the central density than to the parameterization of the density profile. Although a central density of 30 g cm^{-3} may be reasonable for a normal $4M_\odot$ main sequence star,[29] the

structure of a $4M_\odot$ star with a companion neutron star orbiting at a distance of order its radius may well be quite different. We have calculated neutrino absorption with different central densities (and the results are qualitatively similar). In principle the absorption also depends upon the mass of the companion; for normal main sequence stars the density profiles are rather similar, i.e., a function of r/R and the central density only, and $R \propto M^{0.6}$. This implies that $\int n(x)dx \propto M^{0.2}$ is rather insensitive to the mass of the star.

The effect of absorption of neutrinos is shown in Figure 4. At energies above 100 TeV, the absorption cross section is relatively energy independent, so all energies above 100 TeV will have the same phase structure for the relative intensity. The predicted neutrino 'light curves' are shown in Fig. 5.

We now return to the question of whether or not the K's and π's decay in flight. The decay distance (λ_D) of $\pi^\pm$'s and $K^\pm$'s in the star frame is

$$\begin{aligned}(\gamma c\tau)_{\pi^\pm} &= 5.3\times10^6 E_{TeV}\ \text{cm} \\ (\gamma c\tau)_{K^\pm} &= 7.5\times10^5 E_{TeV}\ \text{cm}\end{aligned} \tag{22}$$

The cross section for (π,K) interaction is $\sigma_I \simeq 3\times10^{-26}\ \text{cm}^2$ at high energies ($\gtrsim$ TeV) and so the interaction distance is

$$\lambda_I = (n\sigma_I)^{-1} = 6\times10^7/\rho_{-6}\ \text{cm} \tag{23}$$

where $\rho_{-6} = \rho/10^{-6}\text{cm}^{-3}$. Since the decay length is less than the scale height for density change in the star we have assumed a constant density

in Eq. (23).[30]

There will be a cutoff energy, above which mesons will interact before decaying. We estimate this energy by setting $3\lambda_I = \lambda_D$. This critical energy is given by

$$\begin{aligned} E_c &\simeq 300/\rho_{-6} \text{ TeV} \qquad (K^{\pm}) \\ &\simeq 30/\rho_{-6} \text{ TeV} \qquad (\pi^{\pm}) \ . \end{aligned} \tag{24}$$

Therefore the source function for neutrinos produced by K's and π's should be cut off at an energy of the order of $E_c \simeq 100/\rho_{-6}$ TeV. The cutoff energy is most sensitive to the density in the envelope of the star. By detection of E_c it is possible to gain information about the density in the envelope. In addition to π's and K's, charm and other heavy flavors will be produced. The lifetimes of D and F charmed mesons are less than 10^{-12} seconds, and they will decay 'promptly' and produce neutrinos before interacting. At energies greater than E_c the neutrino flux will be due to 'prompt decays' (as in a 'beam dump' type experiment). However the efficiency for charm and heavy flavor production is expected to be 10^{-2} to 10^{-3} that of π,K production. Therefore above E_c the flux of neutrinos will be suppressed by 10^2-10^3.

Some fraction of the π's and K's initially more energetic than E_c will interact and have their energy degraded to less than E_c before they decay or are absorbed. Once the energy of a π or K has been reduced to the order of E_c it will on average decay before interacting again. Thus we expect some 'piling up' of those π's and K's initially more energetic than E_c at an energy $\simeq E_c$, in turn leading to more decay neutrinos of energy E_c. If the initial spectrum of π's and K's decreases with energy

this will be a small effect (at most order unity). However, if the initial spectrum of π's and K's is approximately monoenergetic this could be a very important effect--as we will discuss in the next section.

We can now relate dN_ν/dE to dN_γ/dE. Using the observed photon spectrum from Eq. (17), we infer the phase-averaged neutrino spectrum (for $E \leq E_c$).

$$\frac{dN_\nu}{dE_{TeV}} \approx \frac{(1-m_\mu^2/m_\pi^2)^{1.1}}{2} \frac{(\Delta\psi)_\nu}{(\Delta\psi)_\gamma} \frac{dN_\gamma}{dE_{TeV}} \quad . \tag{25}$$

Although $(\Delta\psi)_\nu$ is energy dependent, $(\Delta\psi)_\nu \approx 0.4$ is a good approximation for all energies. Therefore

$$dN_\nu/dE_{TeV} \approx 4\times10^{-10}\ E_{TeV}^{-2.1}\ cm^{-2}s^{-1} \quad (E < E_c) \tag{26}$$

and about 10^2-10^3 times smaller for $E > E_c$. We note that the normalization of the predicted neutrino spectrum is uncertain by at least a factor of order 10, due to uncertainties in $\Delta\psi_\gamma$, the photon spectrum, and the possibility of some absorption of UHE photons even during the bright phase. [In fact it is very likely that there is some photon absorption, since a column density of order 60 gcm^{-2} is needed to produce pions, while a column density of only about 20 gcm^{-2} is needed for UHE photons to be absorbed.] In the next section we use this result to calculate count rates in large, underground detectors.

(c) Prospects for Detection in Large, Underground Detectors

Consider a large (of the order of 1000 m^3), underground (distance d below the surface) detector, shown schematically in Fig. 6. For example, the IMB proton decay detector[31] is 23m × 18m × 17m and 1500 m.w.e. below ground. Such a detector can detect neutrinos which: (1) interact within the detector or (2) produce muons in the surrounding rock which have sufficient energy to get to and pass through the detector. We will call the first type of event a 'contained' event and the second type of event a 'muon' event.

The probability that a neutrino which is passing through the detector interacts in the detector is

$$\begin{aligned} P_c(E) &\simeq n\,\sigma\,\ell \quad , \\ &\simeq 4\times10^{-9}\ell_{10}E_{TeV} \quad (E \lesssim 100 \text{ TeV}), \\ &\simeq 7\times10^{-8}\ell_{10}\ell n\, E_{TeV} \quad (E \gtrsim 100 \text{ TeV}) \quad , \end{aligned} \tag{27}$$

where $\ell = \ell_{10}$ 10 m is the typical (water equivalent) linear dimension of the detector,[32] σ is the cross section for $\nu_\mu + N \to \mu^- + X$ [see Eq. (21)] and $n = 6\times10^{23}$ cm^{-3} is the number density of target nuclei.

Relativistic muons lose energy at the rate (per cm water equivalent)[33]

$$-dE/dx \simeq 1.9\times10^{-6}\text{TeV cm}^{-1} + 4\times10^{-6}\text{ cm}^{-1}\,E \tag{28}$$

Integrating this we find that the range of a relativistic muon is

$$L(E) \simeq 3\times10^{5}\text{cm}\ \ell n(1+2E_\mu/\text{TeV}) \quad ,$$

(29)

$$\approx 5\times10^{5}\text{cm}\ E_{\mu}/\text{TeV} \qquad (E_{\mu} \lesssim 1\ \text{TeV})$$

which rises linearly with energy up to an energy of about a TeV and only logarithmically thereafter. Muons produced within a distance $L(E_{\mu})$ of the detector will have sufficient energy to make it to the detector. Thus the effective linear size of the detector for muon type events is $L(E_{\mu})$. Of course, this size can be no larger than the distance from the detector to the earth's surface x (see Fig. 6). The probability that a neutrino of energy E_{TeV} TeV interacts in the rock outside the detector and produces a muon which passes through the detector is

$$P_{\mu}(E_{TeV}) = \int_{o}^{E_{TeV}} \eta\ o(E_{\mu})L(E_{\mu})f(E_{\mu})dE_{\mu}\ , \tag{30}$$

$$\approx 1.\times10^{-6}E_{TeV}[\ell n(1+E_{TeV})]$$

where $f(E_{\mu})dE_{\mu}$ is the probability that the muon produced has an energy between E_{μ} and $E_{\mu}+dE_{\mu}$. For simplicity we have assumed that the typical muon energy is about equal to half that of the incident neutrino.[34] Notice that the ratio P_{μ}/P_{c} increases with energy, and for neutrinos more energetic than a few ℓ_{10} GeV the effective size of the detector for muon events is larger than that for contained events. Thus if the neutrinos are predominantly very high energy (> TeV) the contained type events should be rare.

The event rate in the detector is given in terms of the neutrino spectrum dN_{ν}/dE and the probability P(E) that a neutrino of energy E interacts:

$$\Gamma_i = \text{Area} \times \int P_i(E)\, dN_\nu/dE\, dE \quad , \tag{31}$$

where 'Area' is the cross sectional area presented by the detector. We assume a differential spectrum of the form: $dN_\nu/dE = A\, E_{TeV}^{-n}$. For a spectral index $n < 3$ the muon events are dominated by the highest energy events. The integral in Eq. (31) is cutoff by the logarithmic dependence of L(E) for E > few TeV, or the cutoff in the spectrum discussed in the previous section, E_c, if E_c is less than a few TeV:

$$\Gamma_\mu = \text{Area} \times A \times 1.\times 10^{-6} \int E_{TeV}^{-n+1}\, \ell n(1+E_{TeV})\, dE_{TeV}$$

$$\approx \text{Area} \times A \times 1.\times 10^{-6} \times \int (u-1)^{-n+1}\, \ell n\, u\, du \tag{32}$$

where $u = 1 + E_{TeV}$. The dimensionless integral in Eqn. (32) has the values 200, 20, 14, 5., 4.5 for n = 1.5, 2, 2.1, 2.5, 2.75. Half the contribution to the integral comes from neutrino events with energies between 3-100 TeV.

The contained events on the other hand are dominated by the low energy events (as long as n > 2):

$$\Gamma_c \approx \text{Area} \times \ell_{10} \times A \times 4\times 10^{-9} \int E_{TeV}^{-n+1}\, dE_{TeV}, \tag{33}$$

$$\approx \text{Area} \times \ell_{10} \times A \times 4\times 10^{-9}\, 10^{3(n-2)}\, (E_{min}/GeV)^{-n+2},$$

where E_{min} is the larger of the detector threshold and the low energy cutoff in the neutrino spectrum. The ratio of the two types of events is given by

$$\Gamma_\mu/\Gamma_c \approx 4000\ (1000)^{2-n}\ \ell_{10}^{-1}\ [\int (u-1)^{-n+1} \ell n\ u/10](E_{min}/GeV)^{n-2}. \quad (34)$$

For the neutrino spectrum derived from the high energy photon spectrum ($A \approx 4 \times 10^{-10} cm^{-2} sec^{-1}$ and $n = 2.1$) and a detector cross section of order 4×10^6 cm^2 the predicted event rate for the muon events is

$$\Gamma_\mu \approx 3 \times 10^{-8}\ (Area/4 \times 10^6 cm^2) Hz \quad , \quad (35)$$

or about 1 event per year. Recall that the normalization A could easily be larger by a factor of 10 due to uncertainties in the photon flux, the photon duty cycle, or photon absorption.

This event rate should be compared to the muon background due to cosmic ray interactions in the atmosphere. Using a measured integrated muon flux at the Earth's surface of:

$$N_\mu(>E) \sim 10^{-7}\ E^{-2}\ cm^{-2}\ sr^{-1}\ sec^{-1}, \quad (36)$$

we show the estimated muon background as a function of zenith angle (or slant depth d_3 = d/ 3 km we) in Fig. (7). For IMB this rate is approximately:

$$d\Gamma/d\Omega \sim 5 \times 10^{-4}\ /(\exp(0.5/\cos(\Upsilon)) - 1)^2\ \ Hz\ deg^{-2}\ . \quad (37)$$

The zenith angle of Cygnus X-3 varies between $\theta-\delta$ and $180°-(\theta+\delta)$ with the sidereal period, where $\delta = 40.8°$ is the declination of Cygnus and θ is the latitude of the detector. For IMB θ is 41.5°N so that Cygnus X-3 only gets about 8° below the horizon.[36] As far as background goes the deeper, more southern detectors such as the Kolar Gold Field (θ=12°N) and the Case-Wit-Irvine mine (θ=26.5°S) are much better off.

For completeness, consider the possibility that the neutrino spectrum is steeper than E^{-3}, in which case both the 'contained' and 'muon' events are dominated by the low energy neutrinos.

$$\Gamma_\mu = \text{Area} \times A \times 3\times10^{-9}(E_{min}/\text{GeV})^{-n+3}\ 10^{3(n-2)}/(n-3)\ , \qquad (38)$$

$$\Gamma_c = \text{Area} \times A \times \ell_{10}4\times10^{-9}\ (E_{min}/\text{GeV})^{-n+2}10^{3(n-2)}/(n-2). \qquad (39)$$

In this case the two rates are comparable, and the signal is unlikely to be detectable unless the flux of GeV neutrinos is many orders-of-magnitude greater than that of the photons, which in turn would imply an energy output in neutrinos much greater than 10^{38}ergs sec^{-1}. We should emphasize this point; since the probability for a neutrino to produce a 'muon' event varies either as E^2 (for $E <$ few TeV) or as $E\ell n(E)$ (for $E >$ few TeV) and the neutrino luminosity only varies linearly with neutrino energy, the power required to produce a given event rate in the detector <u>decreases</u> with neutrino energy.

Finally, consider the Hillas model[37] where the observed photon flux is due to the electromagnetic shower produced by a mono-energetic beam of 10^5TeV protons with luminosity of $\approx10^{39}$erg sec^{-1} which hits the

companion star. In this model we would expect an approximately mono-energetic flux of neutrinos of energy a few $\times$ 10^4TeV, assuming that E_c is greater than 10^4 TeV. Assuming that about 10% of the beam energy goes into neutrinos of average energy 10^4 TeV, the resulting neutrino flux is:

$$N_\nu \approx (1/10)\ 10^{39}\text{erg sec}^{-1}\ (\langle E_\nu \rangle \approx 10^4\text{TeV})^{-1}(4\pi r^2)^{-1}$$
$$\approx 10^{-12}\text{cm}^{-2}\text{s}^{-1}\ , \tag{40}$$

Such a flux produces a muon event rate of

$$\Gamma_\mu \approx 10^{-8}\ \text{Hz}\ (\text{Area}/4\times 10^6\text{cm}^2). \tag{41}$$

More likely is the case that $E_c \leq 10^4$TeV, so that the flux of 10^4TeV neutrinos is due to 'prompt' charm and heavy flavor decays and is a factor of 100-1000 smaller than the above estimate, resulting in an event rate which is 10^{-2}-10^{-3} of the above estimate. However, due to the fact that some reasonable fraction of the π's and K's that are produced will interact and lose energy until $E \leq E_c$ and they can decay in flight, a significant fraction, $f \approx 10^{-1}$-10^{-2}, of the 10^{39} erg sec^{-1} should come out in neutrinos of energy of the order of E_c (the pile up effect we discussed in the previous section). In this case

$$N_\nu \approx f \times 10^{39}\text{erg sec}^{-1} \times (E_c)^{-1}(4\pi r^2)^{-1}$$
$$\approx 10^{-9}(f/10^{-1})(E_c/10\text{TeV})^{-1}\ \text{cm}^{-2}\ \text{sec}^{-1}. \tag{42}$$

This leads to a 'muon' event rate of

$$\Gamma_\mu = \text{Area} \times N_\nu \times P_\mu(E_c)$$

$$= 10^{-7}\text{Hz}\ (\text{Area}/4\times10^6\text{cm}^2)(f/10^{-1}) \times \ell n(1+E_c/10\text{TeV}) \qquad (43)$$

Note that for $E_c \gtrsim$ few TeV the predicted event rate is only logarithmically dependent upon E_c. The predicted rate is slightly higher than in the case that $E_c \gtrsim 10^4$TeV because the cross section for $\nu_\mu+N\rightarrow\mu+X$ is still rising linearly with energy at 10 TeV, whereas at energies $\gtrsim$ 100 TeV it rises only logarthmically.

(d) Summary

To summarize, based upon two simple models[15,37] where the high energy gamma rays from Cygnus X-3 are produced by a beam of energetic protons interacting with the envelope of the companion star, we have calculated the expected neutrino flux, normalized to the photon flux. Up to an energy where the pions and kaons whose decays produce the bulk of the neutrinos interact before they have time to decay, the neutrino flux is comparable to the photon flux. At higher energies the neutrino flux is primarily due to charm and heavy flavor decays and the flux is down from that of the photons by a factor of about 100-1000. The source neutrino flux is modulated by absorption of neutrinos by the companion star, resulting in the energy dependent neutrino light curves shown in Fig. 5. Normalizing the predicted neutrino flux to the observed gamma ray flux results in a predicted muon event rate which might be detectable in a large, underground detector like IMB. The predicted

contained event rate is about a 1000 times smaller. Most of the muon events are due to neutrinos of energy of 3-100 TeV and so should be heavy track. The predicted event rate could be significantly larger if the photon duty cycle is less than 5% or if there is significant absorption of UHE γ-rays within the system.

If the spectrum of neutrinos is not $\propto E^{-2.1}$ as the present UHE γ-ray data suggests, and is steeper than E^{-3}, then the number of contained and muon events will be comparable and dominated by GeV neutrinos. However, unless the flux of GeV neutrinos is many orders-of-magnitude greater than that of photons, the neutrinos will not be detectable in large proton decay detectors.

Finally, we should mention that if other very robust binary X-ray sources such as Vela X-1, LMC X-4, and Her X-1 are also potent sources of UHE γ-rays,[38] then they should produce high energy neutrinos in a similar fashion. In particular, recent observations of the UHE γ-ray spectrum of Vela X-1[39] and TeV γ-rays from Her X-1[40] indicate fluxes which are comparable to that of Cyg X-3, suggesting that Vela X-1 and Her X-1 should produce comparable fluxes of high energy neutrinos. If it is possible to detect neutrinos from systems like Cyg X-3, the neutrino 'light curve' can be used to infer the core density of the companion and E_c can be used to determine the density of the stellar envelope. Probing a system with a many TeV neutrino beam of luminosity 10^{38}erg sec^{-1} offers a multitude of new possibilities.

ACKNOWLEDGEMENTS

T.P.W. wishes to thank his collaborators on the Cyg X-3 work, E.W. Kolb and M.S. Turner.

TABLE AND FIGURE CAPTIONS

Table I: A compilation of Γ's for $(E_0, E_c) = (1,70)$EeV (increasing E_0 to 10EeV decreases the bright phase rates by $\sim 10^3$, but has little effect on the minimum rates). We list the minimum rate, R_h/R_L (~20) times the minimum rate, and R_H/R_L times the bright phase for $\bar{z}=2,4$, and 7.

	Minimum (xR_H/R_L)	Bright Phase ($\bar{z}=2,4,7$)
Γ_{down}(DUMAND)	$10^{-5}(2\times10^{-4})$ yr^{-1}	2×10^{-4}, $^{-2}$, 0 yr^{-1}
Γ_{up}(Fly's Eye)	$10^{-6}(2\times10^{-5})$ yr^{-1}	2×10^{-5}, $^{-3}$, $^{-1}$ yr^{-1}

Figure (1): The superposition of evolved $E^{-2.5}$ extragalactic spectra and an E^{-30} local spectrum for 6 and 48 interaction lengths. Solid curves are fit to low energy ($<10^{19}$eV) data while the dashed curve is a 6 IL fit to the peak at 5×10^{19}eV. The dotted curve assumes a local E^{-3} component due to the superposition of large z sources. The Fly's Eye data is shown with error bars.

Figure (2): Bright phase differential neutrino spectra normalized so that $j_o(E) = 1$ at 10^{17}eV.

Figure (3): A schematic diagram of the Cyg X-3 system. The dashed circle shows the atmosphere, y is the distance between the pulsar and the surface of the companion star, ψ is the phase angle, and θ is the angle between the line-of-sight and the line which connects the intersection of the line-of-sight with the star and the center of the star. We have omitted the shroud from this diagram and have assumed that the line-of-sight lies in the orbital plane.

Figure (4): – The neutrino cutoff energy E_{cutoff}, determined by $\int n(x)\sigma(E_{cutoff})dx = 1$, as a function of θ (see Fig. 1), computed for a $4\ M_{\odot}$ star.

Figure (5): – The neutrino 'light curve' for different neutrino energies. In constructing the 'light curve' we have assumed that $i = 90°$ and $y/R \ll 1$ so that $\theta = \psi$ (see Fig. 1 and footnote 11). Since the muon events in an underground detector are primarily due to neutrinos of energy of order 10 TeV, that is the 'light curve' which would be observed.

Figure (6) - Schematic diagram of the detector. The distance below the surface is d, the zenith angle of Cyg X-3 is Υ, and the distance to the surface at zenith angle Υ is x.

Figure (7): – The approximate background atmospheric muon rate [see Eq. (3.11)] as a function of $d_3/\cos\Upsilon = x_3 = x/3$ km. The scales on the top and right hand side are those appropriate for a detector at a depth $d = 1500$ m.w.e. with cross section of 4×10^6 cm^2.

References

1. C. T. Hill and D. N. Schramm, Phys. Rev. D31, 564 (1985); Phys. Lett. 131B, 247 (1983).
2. C. T. Hill, D. N. Schramm, and T. P. Walker, Fermilab-Pub-85/143-THY (1985), submitted to Phys. Rev. Lett.
3. T. K. Gaisser and T. Stanev, Phys. Rev. Lett. 54, 2265 (1985); V. S. Berezinsky, C. Castagnoli, and P. Galeotti, Instituto de Fisica Generale dell' Universita di Torino report, 1985; G. Cocconi, CERN report, 1985; A. Dar, Phys. Lett. 159B, 102 (1985).
4. E. W. Kolb, M. S. Turner, and T. P. Walker, Phys. Rev. D32, 1145 (1985).
5. R. M. Baltrusaitis, et. al., Phys. Rev. Letters 54, 1875 (1985).
6. K. Greisen, Phys. Rev. Letters 16, 748 (1966).
7. V. A. Kuzmin, G. T. Zatsepin, Zh. Eksp. Teor. Fiz. 4, 78 (1966).
8. See the useful review of J. Linsley in "Origin of Cosmic Rays" 53-68, ed. Setti, et. al., (1981) and refs. therein. Also, A. M. Hillas, Phys. Reports 20C, 59 (1975); F. Stecker, Phys. Rev. Letters 21, 1016 (1968); Comments, Astrophys., Vol. 7, No. 4, pp. 129, (1978); The Astrophysics Journal 228, 919 (1979); V. Berezinsky, G. T. Zatsepin, Sov. J. Nucl. Phys. 11, 111 (1970) and V. Berezinsky, V. Ginzburg, L. Ozernoy, cont. to Dumand '80 and '78G; F. Stecker, in Proc. Neutrino '79, 475; R. Partridge, P. J. E. Peebles, Ap. J. 147, 868 (1967).
9. G. Blumenthal, Phys. Rev. D1, 1596, (1970); see also E. Freenberg and H. Primakoff, Phys. Rev. 73, 449 (1948).

10. C. T. Hill, D. N. Schramm, contributions to 18th ICRC (Bangalore) (1983).

11. D. Koo, talk presented at "Structure and Evolution of Active Galactid Nuclei", Trieste, Italy (April, 1985).

12. A. Szalay, private communication.

13. D. Koo, Proceedings of the Erice Workshop on "The Spectral Evolution of Galaxies", eds. C. Chiosi, A. Renzini, Dordrecht, Reidel (1985).

14. D. R. Parsignault, et. al. Ap. J. 218, 232 (1977).

15. W. T. Vestrand and D. Eichler, Ap. J. 261, 251 (1982).

16. M. Milgrom, Astr. Ap. 51, 215 (1976).

17. P. Hertz, P. Joss, and S. Rappaport, Ap. J. 224, 614 (1978).

18. R. C. Lamb, C. E. Fichtel, R. C. Hartman, D. A. Kniffen, and D. J. Thomson, Ap. J. 212, L63 (1977).

19. Yu. I. Neshpor, et. al., Ap. Space Sci. 61, 349 (1979).

20. S. Danaher, D. J. Fegan, N. A. Porter, and T. C. Weeks, Nature 289, 568 (1981).

21. R. C. Lamb, C. P. Godfrey, W. A. Wheaton, and T. Turner, Nature 296, 543 (1982).

22. M. Samorski and W. Stamm, Ap. J. 268, L17 (1983); J. Lloyd-Evans, R. Coy, A. Lambert, J. Lapikens, M. Patel, R. Reid, and A. Watson, Nature 305, 784 (1983).

23. J. M. Dickey, Ap. J. 273, L71 (1983).

24. The observations suggest that the angle i between the normal to the orbital plane and the line-of-sight is about 90° and that the distance between the pulsar and the companion star y is much less than R. If this is so, then θ, the angle between the point where

the line-of-sight intersects the companion star and a line connecting that point to the center of the star, is equal to the phase angle ψ (see Fig. 1). The angle θ determines when the UHE γ-ray pulses should occur ($\theta \simeq \pm \pi/2$) and the degree of neutrino absorption. For $i \neq 90°$ and $y \neq 0$, θ and ψ are related by: $\sin\theta = (1+y/R)(\cos^2 i + \sin^2 i \sin^2\psi)^{1/2}$, which has the limiting forms: $\sin\theta = (1+y/R)\sin\psi$, for $i = 90°$; and $\cos\theta = \sin i \cos\psi$, for $y/R \ll 1$. Throughout this paper we have assumed that $i = 90°$ and $y \ll R$.

25. D. Eichler, Nature 275, 725 (1978).

26. The astrophysical production of UHE γ and ν_μ's from π-decays and the possible detection of the ν's has been considered in more generality by V. Stenger, Astrophys. J. 284, 810 (1984); also see references therein.

27. See also, F. W. Stecker, Ap. J. 228, 919 (1979).

28. Yu. M. Andreev, V. S. Berezinsky, and A. Yu. Smirnov, Phys. Lett. 84B, 247 (1979).

29. See, for example, D. Clayton, Principles of Stellar Evolution and Nucleosynthesis (McGraw-Hill: New York, 1968).

30. In the text we have treated the interaction of the proton beam with the envelope of the star in a highly simplified way. A star being bombarded by 10^{38}-10^{39} erg sec^{-1} is not likely to resemble an ordinary star; however, for an ordinary star this problem can be treated much more precisely. In an ordinary star the amount of material above the photosphere (the shell in the star where the temperature equals the effective temperature of the star) is negligible, $\int_{R_{Tn}}^{\infty}\rho d\ell \simeq$ few g cm^{-2}. Below the photosphere, in the envelope, $\rho \sim pn$ ($n=3.25$ for a radiative envelope, appropriate for

stars more massive than about 1.5 $M_\odot$; n=1.5 for a convective envelope, appropriate for stars less massive than about 1.5 $M_\odot$). The equations of hydrostatic equilibrium then imply a density run in the envelope: $\rho = \rho_o(d/h+1)^n$, where d is the depth below the photosphere, h is the scale height $\simeq$ few $\times 10^8$ cm, and ρ_o is the density at the photosphere $\simeq 10^{-7}$ g cm^{-3}. From this one can compute that: $\int_o^d \rho d\ell \simeq \rho_o h[(d/h+1)^{n+1}-1]/(n+1)$. It then follows that $\int_o^d \rho d\ell \simeq 100$ g cm^{-2} at a depth d $\simeq$ 2h, and that $\int \rho d\ell$ has increased by another 100 g cm^{-2} at a depth d $\simeq$ 3h. This means that π's and K's which are produced in the first 100 g cm^{-2} have to traverse roughly a scale height ($\simeq 10^8$cm) before they encounter another 100 g cm^{-2}. For a discussion of stellar envelopes, see e.g., M. Schwarzschild, The Structure and Evolution of the Stars (Dover: N.Y., 1958).

31. R. M. Bionta, et. al., AIP Conference Proceedings 96, 138 (1983).

32. For convenience we have expressed all distances in their water equivalent values, i.e., d.w.e. = d(ρ/1 g cm^{-3}).

33. B. B. Rossi, High Energy Particles (New York: Prentice-Hall, 1952); L. B. Bezrukov and E. V. Bugaev, ICRC 17, MN102.

34. There is an additional small background of through-going muons due to atmospherically-produced neutrinos which interact in the rock surrounding the detector. Their flux is roughly isotropic. The rate for muons with energy greater than 2 GeV is $\simeq 8 \times 10^{-17}$cm^{-2} deg^{-2}sec^{-1}, and with energy greater than 1 TeV is $\simeq$ 10^{-17}cm^{-2}deg^{-2}sec^{-1}. For further discussion, see T. K. Gaisser and T. Stanev, Phys. Rev. D30, 985 (1984).

35. For $\nu + N \to \mu^- + X$, $d\sigma/dy_2 \simeq$ constant, while for $\bar{\nu} + N \to \mu^+ + X$, $d\sigma/dy \simeq$ constant $\times (1-y)^2$; here $(1-y) = E_\mu/E_\nu$. This means that for

$\nu + N \rightarrow \mu^- + X$, $\langle E_\mu \rangle \approx E_\nu/2$, and for $\bar{\nu} + N \rightarrow \mu^+ + X$, $\langle E_\mu \rangle \approx 3E_\nu/4$. The average range of a muon produced by a neutrino (or antineutrino) of energy E_ν is: $\langle \ell \rangle = \int_0^{d\nu} \ell(E_\mu)(d\sigma/dE_\mu)dE_\mu / \int(d\sigma/dE)dE_\mu$. For neutrino-produced muons: $\langle \ell \rangle \approx \ell(aE_\nu)$, where depending upon E_ν a varies between 0.5 and 0.37; for antineutrino-produced muons: $\langle \ell \rangle \approx \ell(aE_\nu)$, where a varies between 0.72 and 0.75. For simplicity, in Eqn. (3.4) we have taken $\langle \ell \rangle \approx \ell(E_\nu/2)$.

36. The cosine of the zenith angle of Cyg X-3 is given by: $\cos \Upsilon = \sin \theta \sin \delta + \cos \theta \cos \delta \sin [2\pi t/23^h56^m]$, and so Υ varies between $(\theta-\delta)$ and $[180°-(\theta+\delta)]$. With the exception of the Kolar Gold Field detector, all existing large, underground detectors are between 36°N and 46°N latitude, so that Cyg X-3 never gets much below the horizon at any of the detectors.

37. A. M. Hillas, Nature 312, 50 (1984).

38. G. Chanmugam and K. Brecher, Nature 313, 767 (1985).

39. R. J. Protheroe, R. W. Clay, and P. R. Gerhardy, Astrophys. J. 280, L47 (1984).

40. J. C. Dowthwaite, A. B. Harrison, I. W. Kirkman, H. J. Macrae, K. J. Orford, K. E. Turver, and M. Walmsley, Nature 309, 691 (1984).

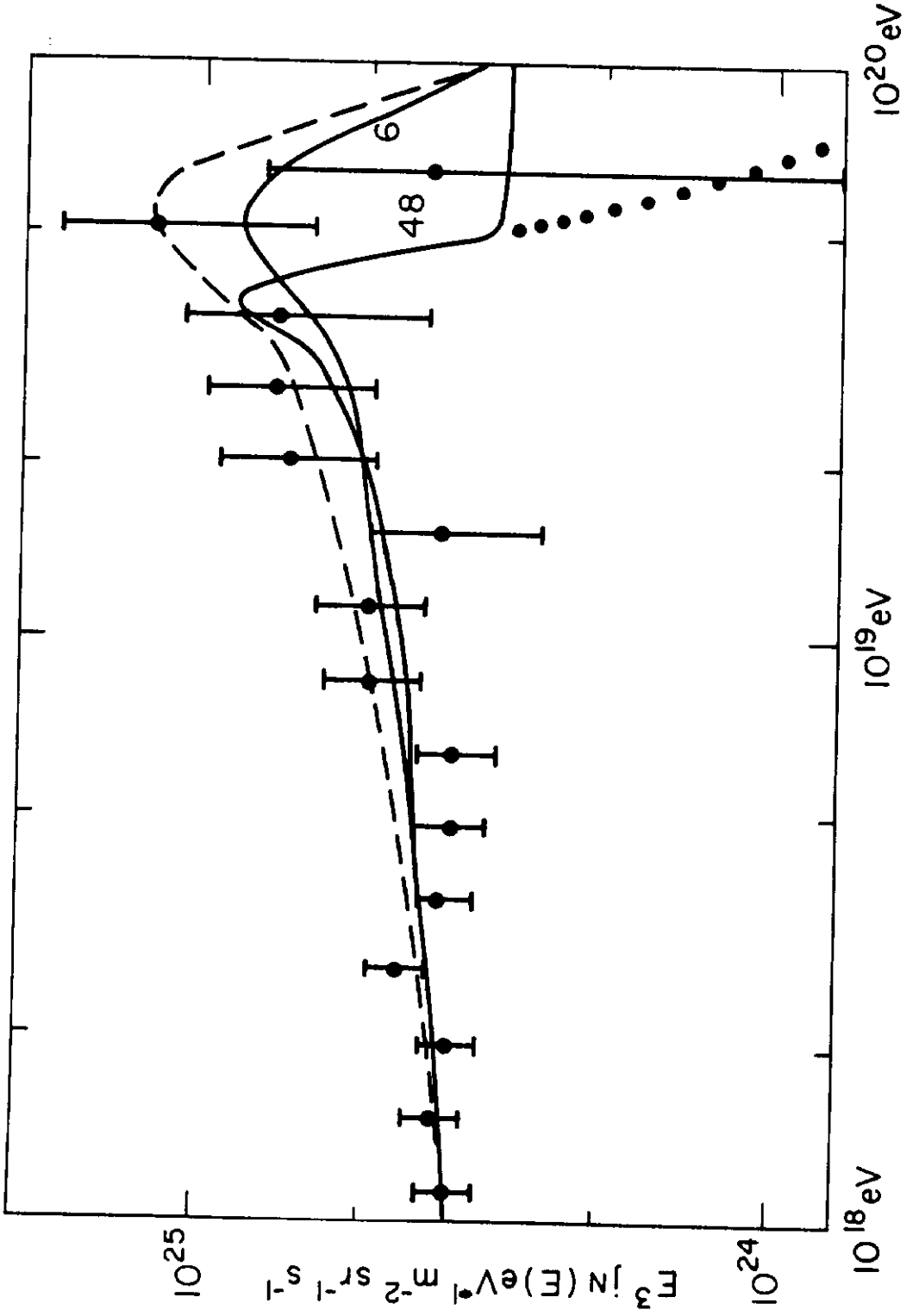

Fig. 1

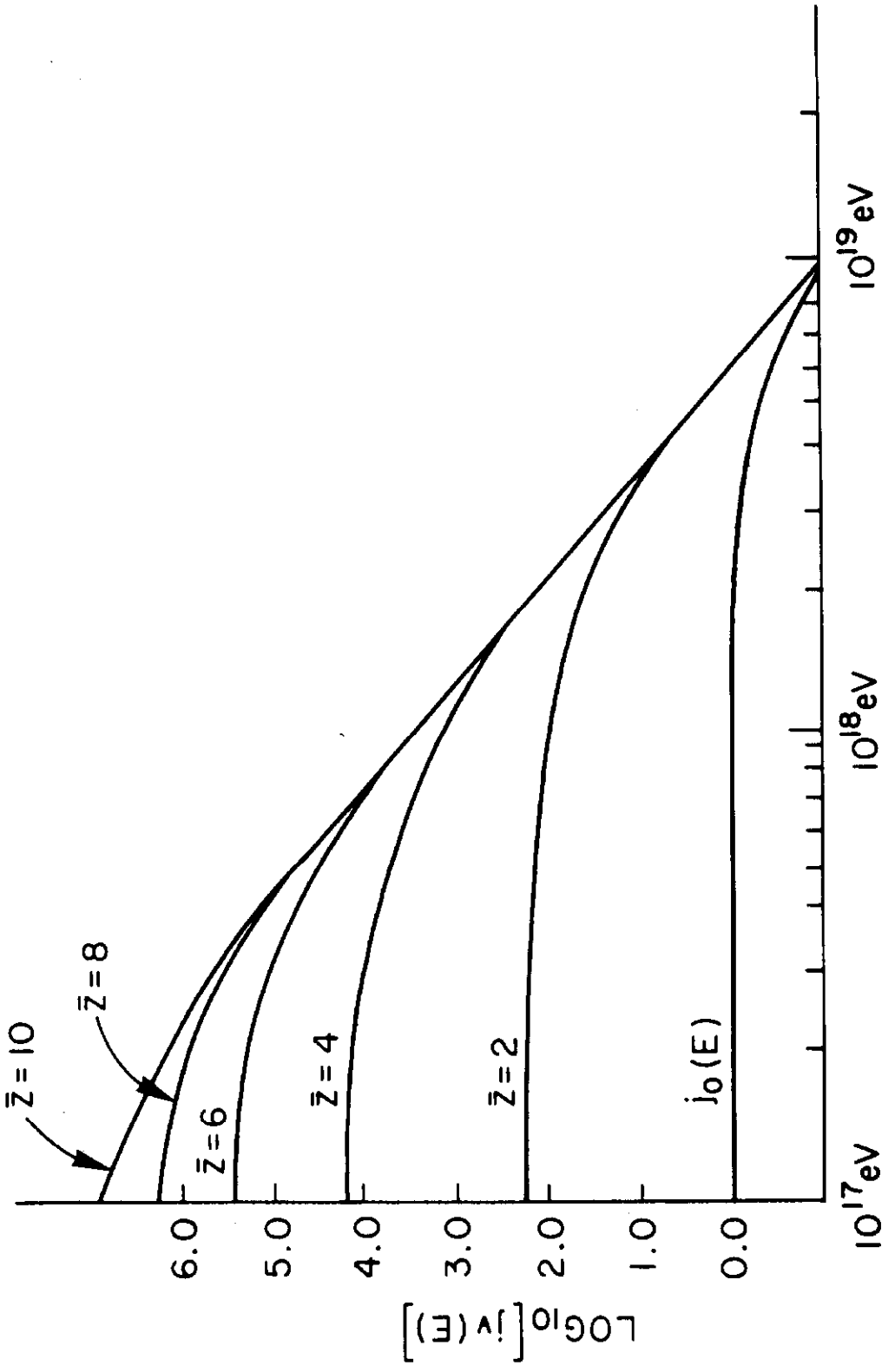
$\log_{10}[j_\nu(E)]$
6.0
5.0
4.0
3.0
2.0
1.0
0.0
10^{17}eV
10^{18}eV
10^{19}eV
$j_0(E)$
$\bar{z}=2$
$\bar{z}=4$
$\bar{z}=6$
$\bar{z}=8$
$\bar{z}=10$

Fig. 2

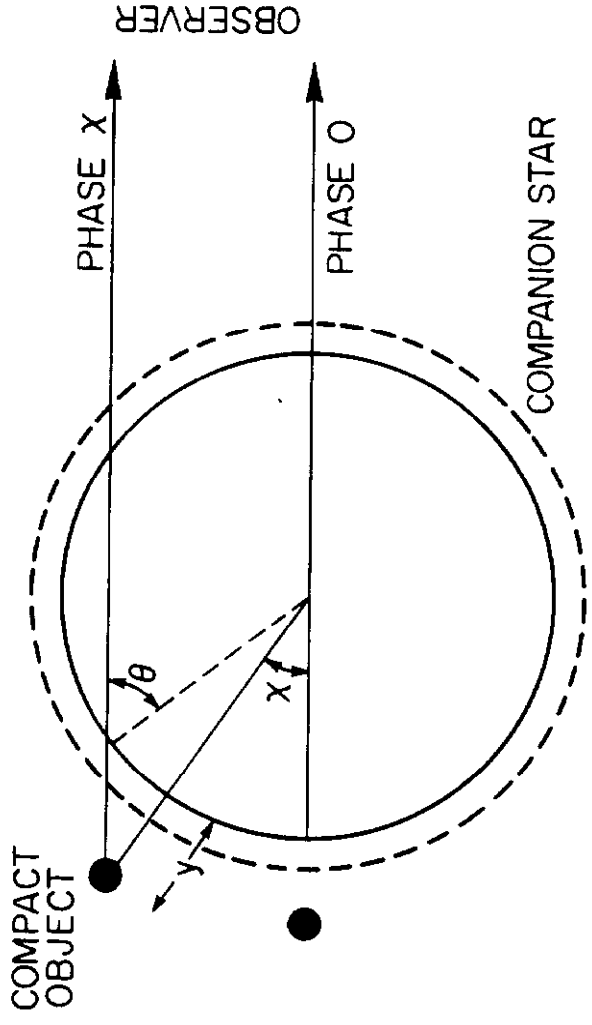

THE CYG X-3 SYSTEM
(Orbital Plane)

Fig. 3

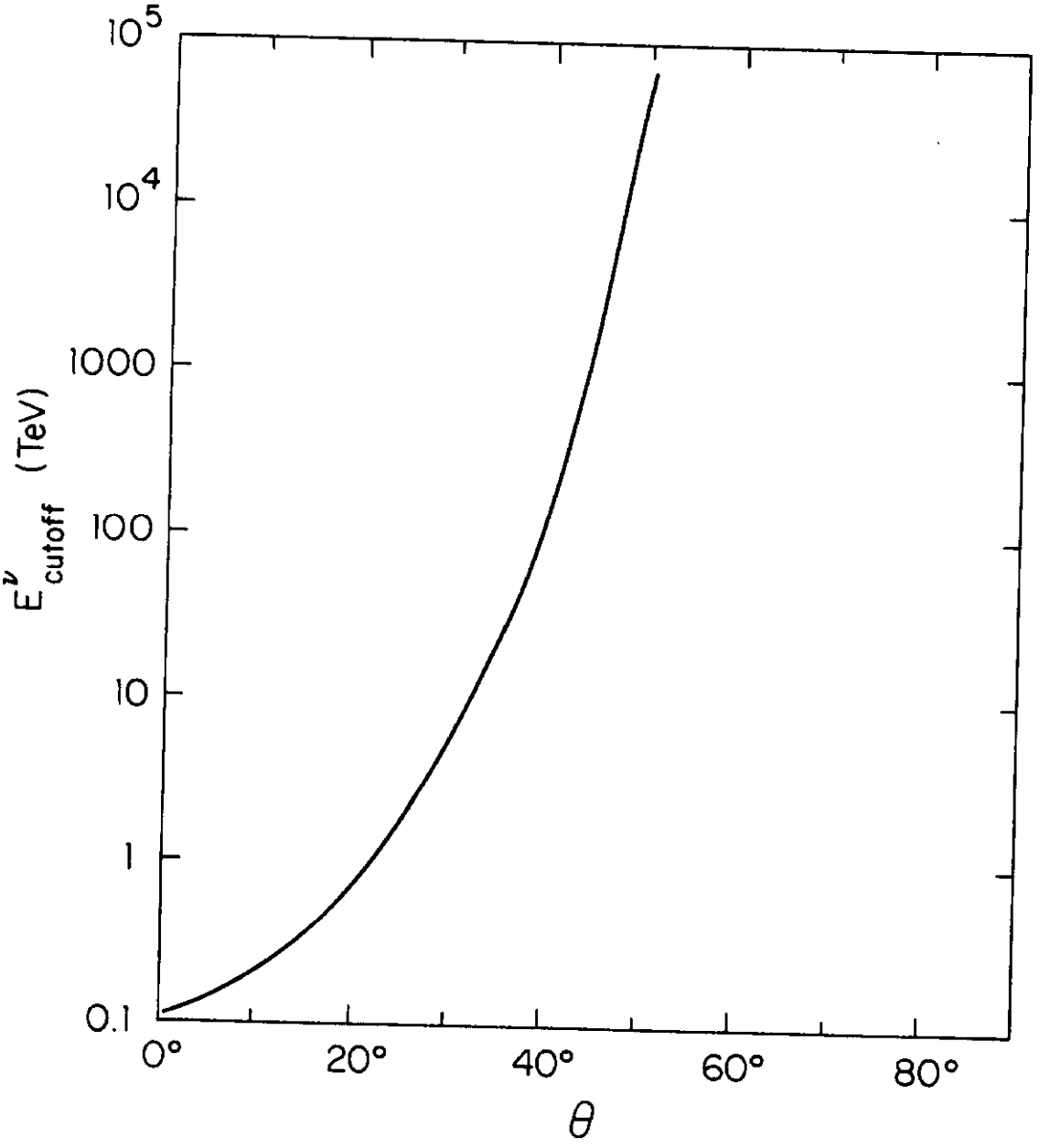

Fig. 4

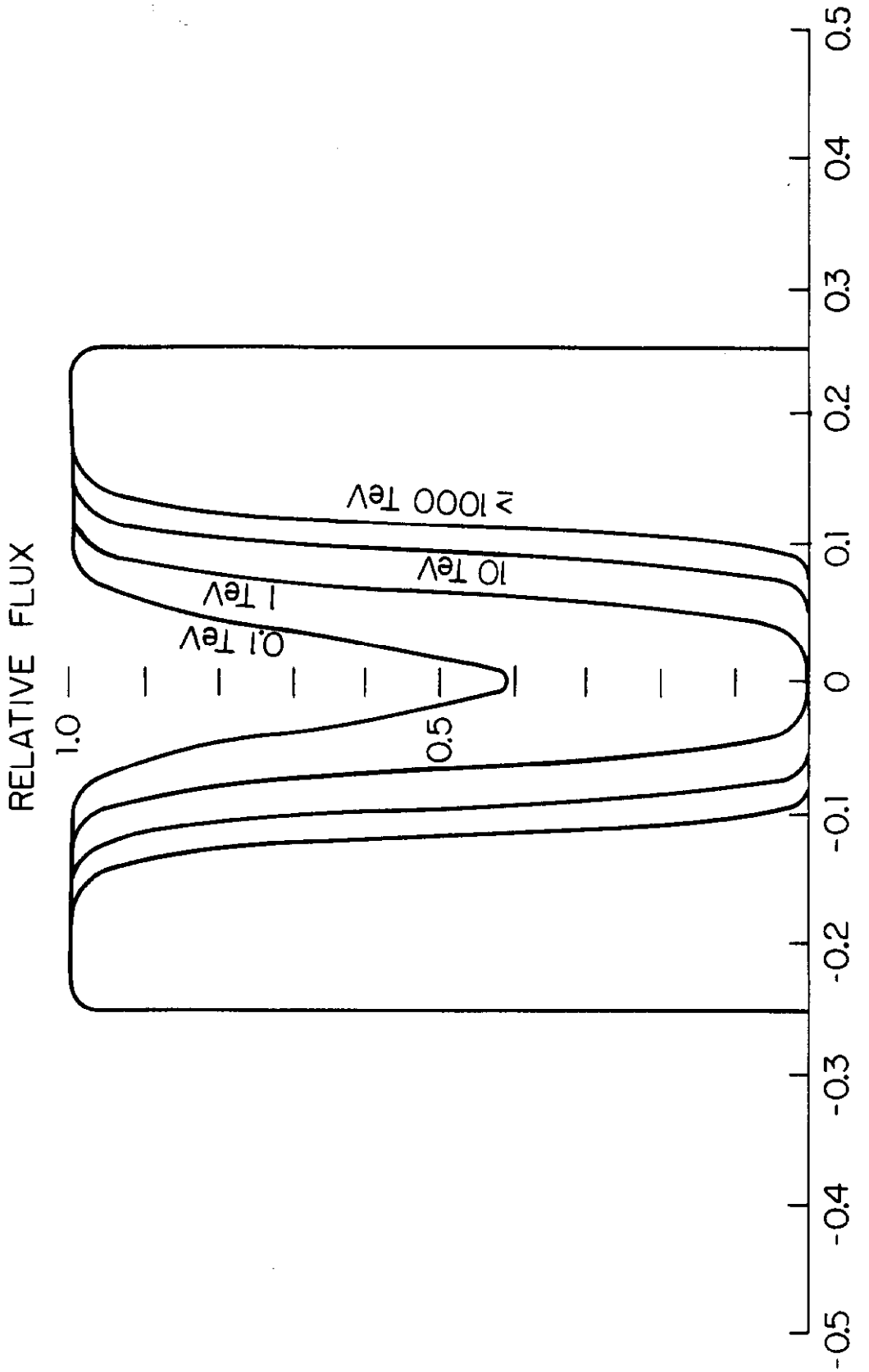
RELATIVE FLUX
1.0
0.5
0.1 TeV
1 TeV
10 TeV
≥ 1000 TeV
-0.5
-0.4
-0.3
-0.2
-0.1
0
0.1
0.2
0.3
0.4
0.5
PHASE ψ

Fig. 5

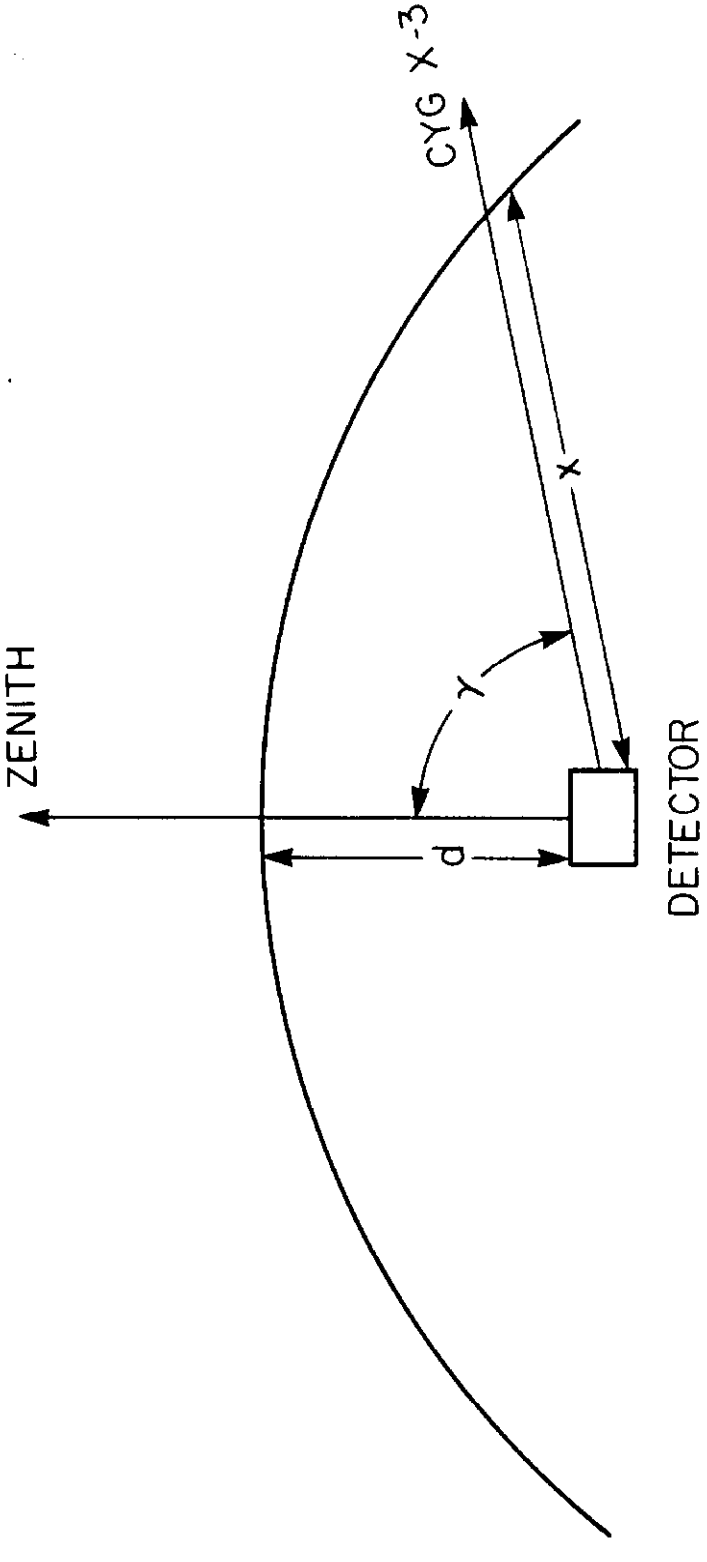

Fig. 6

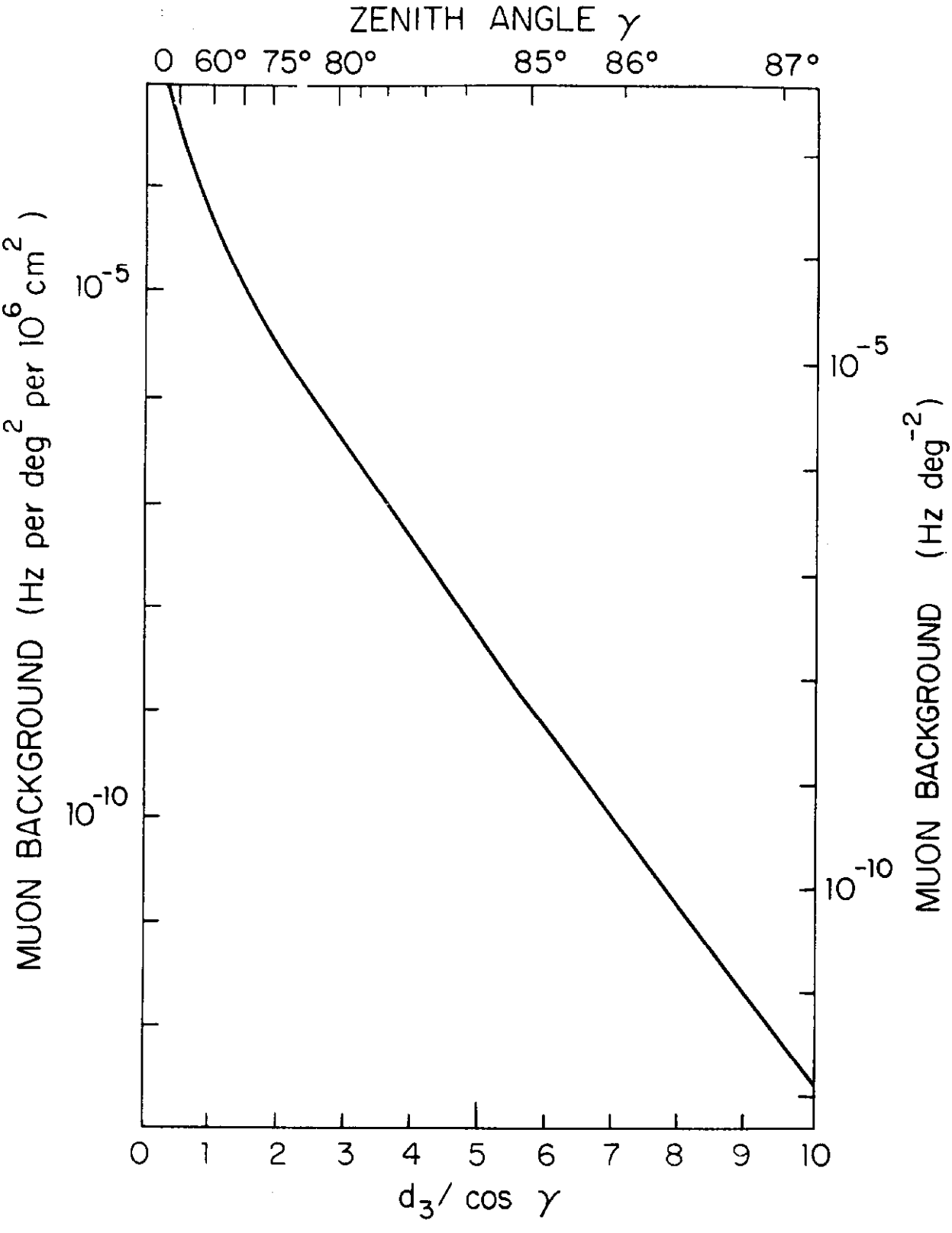
ZENITH ANGLE γ
0 60° 75° 80° 85° 86° 87°
MUON BACKGROUND (Hz per deg² per 10⁶ cm²)
MUON BACKGROUND (Hz deg⁻²)
10⁻⁵
10⁻¹⁰
0 1 2 3 4 5 6 7 8 9 10
d₃/ cos γ

Fig. 7